ICAS-92-2.10.4

A SENSITIVITY ANALYSIS OF THE STABILITY OF A TUG-ROPE-SAILPLANE SYSTEM

Guido de Matteis and Luciano M. de Socio
Department of Mechanics and Aeronautics
University of Rome "La Sapienza"
Rome, Italy

Abstract

This paper concerns an analysis of the stability of a tug–rope–sailplane system from the point of view of the sensitivity of the characteristic modes to changes of the most important system parameters. Both longitudinal and transversal perturbations are considered. The main results concern a distinction between parameters which influence the dynamics of the system and parameters which do not. The effect of the cable characteristics on the motion of the whole system is also discussed.

Nomenclature

A	aspect ratio
$\mathbf{A}$	state matrix
A_c	rope cross section
b	span
c	reference chord
$c.g.$	center of gravity
C_{L_c}, C_{D_c}	aerodynamic coefficients of the rope
$C_{D_{0c}}, k$	force coefficients of the rope
d	rope diameter
E	Young's modulus
f	sag of the rope
F_I, F_V	inertial and body reference frames
$\mathbf{F}$	aerodynamic force on the plane
$\mathbf{F}_c$	aerodynamic force on the rope
$\mathbf{g}$	acceleration of gravity
$\mathbf{I}$	inertia matrix
l	rope length
$\mathbf{L}_{IV}$	transformation matrix from F_V to F_I
m	mass
$\mathbf{n}$	unit vector tangent to the rope
p	parameter of the system
R	radius of curvature
s	curvilinear abscissa
S	reference surface
t	time
$\mathbf{T}$	thrust force
U_e	velocity of F_I
U, V, W	velocity component of the c.g. in F_I
U_c, V_c, W_c	local velocity components of the rope
$\mathbf{U}$	unit matrix
$\mathbf{v}$	velocity
$\mathbf{v}_r$	velocity relative to the flow
x, y, z	local coordinates in F_I
$\mathbf{x}_i$	*right* eigenvector
$\mathbf{y}_i$	*left* eigenvector

Greek symbols

α	angle of attack
γ	rope mass per unit length
Δz	vertical distance between the planes
ϵ	stretching
λ	eigenvalue
ξ, η, ς	coordinates in F_V
ρ	density
σ	real part of λ
τ	tension
φ, ϑ, ψ	Euler angles
$\mathbf{\Phi}$	Euler angle rate vector
ω	coefficient of the imaginary part of λ
$\boldsymbol{\omega}$	angular velocity

Subscripts

A	tow-plane
a	attachment point
B	sailplane
c	cable
G	center of gravity
r	relative
0	unstretched

I. Introduction

In this paper we consider a very peculiar flexible system, the one made of an aircraft which tows a glider. In spite of being a relatively old problem, a really accurate modelling of a tug-rope-sailplane combination appeared only recently(1). The model is able to provide a realistic simulation of the dynamics and an evaluation of the stability of the system and is based on a rigorous mathematical representation of the dynamics of the cable. Other models which appeared even in the recent past, in the pertinent literature, are to different extents effective in describing the most general aspects of the phenomenology. However some stability related questions, which are of foremost importance from the point of view of the flight safety, could not be satisfactorily answered until full consideration was paid to the rope dynamic behaviour. Purpose of this paper is to evaluate those elements of the sensitivity matrix which appear of noticeable interest in applications, by taking advantage of the most recent model.

Various more or less customary definitions can be given of sensitivity. In this regard see, for example, the articles in Ref. 2. Here we refer to the sensitivity matrix which is usually met when dealing with flexible structures, namely the array the elements of which are the derivatives of the eigenvalues of the state matrix with respect to the physical parameters of the system. When we consider our specific problem we have to recall that the greatest influence in providing safe equilibrium configurations of the system is associated to the cable length, to the relative position of the two planes and to the attachment point of the rope to the glider. This was already proved for motions in a vertical plane by evaluating the first significant modes when those quantities are changed[1]. Lately, similar conclusions could be anticipated for some motions out of the longitudinal plane[3].

In what follows we report the full set of basic equations and related boundary conditions which represent the nonlinear mathematical model. Then the equilibrium state is discussed and the linearization procedure leading to the calculation of the eigenvalues of the state matrix is recalled. After indicating the basic parameters for the sensitivity evaluation and the related computational method, several results are reported for the in-plane and the out-plane cases.

II. Analysis

Let us consider the partial differential equation which governs the dynamics of a perfectly flexible cable subjected to its own weight and to the aerodynamic forces. The boundary conditions at the two ends of the rope are expressed by kinematic relations in terms of position and speed of the two planes. Since these quantitites are also unknown the equations for the dynamics of the tug and of the glider are then to be solved as part of the differential problem which corresponds to the mathematical model[1].

In vectorial form we write for an extensible cable of uniform density and geometry

$$\gamma \frac{\partial \mathbf{v}_c}{\partial t} = \frac{\partial}{\partial s}(|\tau| \mathbf{n}) + \mathbf{F}_c + \gamma \mathbf{g} \tag{1}$$

where γ is the mass per unit length, τ is the tension force, $\mathbf{v}_c = (U_c, V_c, W_c)^T$ is the local velocity vector, $\mathbf{F}_c$ is the aerodynamic force, $\mathbf{n} = (\partial x/\partial s, \partial y/\partial s, \partial z/\partial s)^T$ is the unit

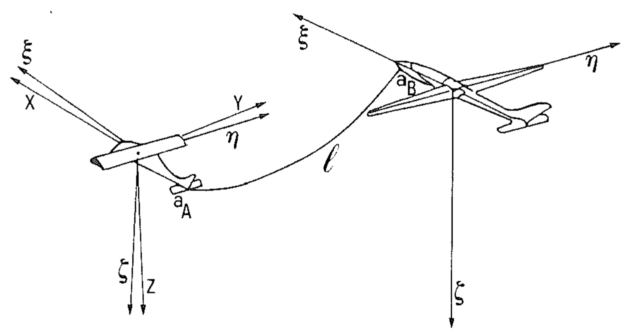

Fig. 1 - Sketch of the system

vector locally tangent to the rope, $\mathbf{g}$ is the acceleration of gravity and s is the intrinsic coordinate along the cable length. The aerodynamic force acting on an element of the cable is given by[4]

$$\mathbf{F}_c = \frac{1}{2}\rho d \left[C_{L_c} \tilde{\mathbf{v}}_{r_c} (\tilde{\mathbf{v}}_{r_c} \mathbf{n}) + C_{D_c} |\mathbf{v}_{r_c}| \mathbf{v}_{r_c}\right] \tag{2}$$

where d is the cable diameter and the operator $\sim$ is used for the cross products (i.e. $\mathbf{v}_{r_c} \wedge \mathbf{n} = \tilde{\mathbf{v}}_{r_c}\mathbf{n}$)[5]. The local velocity relative to the air is $\tilde{\mathbf{v}}_{c_r} = -(U_e + U_c, V_c, W_c)^T$ where U_e is the stationary velocity of the reference system F_I, centered in the tug c.g.[1], with respect to a flat Earth fixed inertial frame (Fig. 1).

The aerodynamic coefficients in Eq. 2 are

$$\begin{aligned} C_{L_c} &= k(1 - \cos^2 \alpha_c) \cos \alpha_c \\ C_{D_c} &= C_{D_{0_c}} + k(1 - \cos^2 \alpha_c)^{3/2} \end{aligned} \tag{3}$$

with $\cos \alpha_c = \mathbf{v}_{r_c} \cdot \mathbf{n} / |\mathbf{v}_{r_c}|$. Finally the tension is $|\tau| = E A_c \epsilon$ where E is the Young's modulus, A_c is the cross section of the rope and the stretching ϵ is

$$\epsilon = \left[\left(\frac{\partial x}{\partial s_0}\right)^2 + \left(\frac{\partial y}{\partial s_0}\right)^2 + \left(\frac{\partial z}{\partial s_0}\right)^2\right]^{1/2} - 1 \tag{4}$$

For the planes we have

$$m_A \mathbf{L}_{VI_A} \dot{\mathbf{v}}_{G_A} = \mathbf{F}_A + \tau_{a_A} + m_A \mathbf{L}_{IV_A} \mathbf{g} + \mathbf{T} \tag{5}$$

$$m_B \mathbf{L}_{VI_B} \dot{\mathbf{v}}_{G_B} = \mathbf{F}_B - \tau_{a_B} + m_B \mathbf{L}_{IV_B} \mathbf{g} \tag{6}$$

and

$$\mathbf{I}_A \dot{\omega}_A + (\tilde{\omega} \mathbf{I} \omega)_A = -(\tilde{r}_a \mathbf{R}_a)_A + \mathbf{M}_A \tag{7}$$

$$\mathbf{I}_B \dot{\omega}_B + (\tilde{\omega} \mathbf{I} \omega)_B = (\tilde{r}_a \mathbf{R}_a)_B + \mathbf{M}_B \tag{8}$$

where subscripts A and B indicate tow-plane and glider respectively, $\mathbf{L}_{VI}$ is the transformation matrix from the inertial frame to the body frame, ω and $\mathbf{v}_G = (U, V, W)$ are the angular and linear velocities of the vehicle, respectively. Furthermore $\mathbf{F}$ and $\mathbf{T}$ are the aerodynamic and thrust forces respectively, $\tau_a = (|\tau| \mathbf{L}_{VI} \mathbf{n})_a$ is the tension force at the attachment point a and $\mathbf{R}_a = (\xi, 0, \varsigma)^T$ is the position vector of a. $\mathbf{M}$ is the aerodynamic moment and $\mathbf{I}$ the inertia matrix of the airplane.

Equations (5)-(8) are formulated in body axes. However, in order to relate these equations to the governing equations of the cable, the velocity components and the coordinates of the airplane are expressed in the inertial frame. As a consequence, the aerodynamic force and moment in Eqs. (5)-(8) are written in term of the c.g. velocity relative to the wind, namely $\mathbf{v}_r = -\mathbf{L}_{VI}(U_e + U, V, W)^T$.

The set of governing equations is completed by the following kinematic relations for the cable coordinates

$$\frac{\partial \mathbf{P}_c}{\partial t}(s) = \mathbf{v}_c(s) \tag{9}$$

where $\mathbf{P}_c = (x, y, z)^T$, by the boundary conditions at the rope ends

$$\frac{d\mathbf{P}_c}{dt} = \mathbf{v}_{G_A} + (\tilde{\omega}\mathbf{L}_{IV}\mathbf{R}_a)_A \qquad \text{for } s=0 \quad (10)$$

$$\frac{d\mathbf{P}_c}{dt} = \mathbf{v}_{G_B} + (\tilde{\omega}\mathbf{L}_{IV}\mathbf{R}_a)_B \qquad \text{for } s=1 \quad (11)$$

and, finally, by the relation for the Euler angle rate vector $\dot{\mathbf{\Phi}}$

$$\dot{\mathbf{\Phi}}_{A,B} = \mathbf{R}^{-1}_{A,B}\omega_{A,B} \qquad (12)$$

where $\dot{\mathbf{\Phi}} = (\dot{\varphi}, \dot{\vartheta}, \dot{\psi})^T$. The expression of the transformation matrix $\mathbf{R}^{-1}$ can be found in Ref. 5.

The fundamental equations can be put in dimensionless form and, in so doing, the characteristic products come into evidence. Among the others, the following numbers are of the foremost importance

$$D_g = \frac{|\mathbf{g}|c_B}{2U_e^2} \quad D_1 = \frac{b_B}{c_B} \quad D_2 = \frac{b_A}{c_A} \quad D_c = \frac{c_B}{c_A}$$
$$D_B = \frac{b_B}{b_A} \quad D_A = \frac{\rho d c_B}{4\gamma} \quad D_D = \frac{c_B}{2l_0} \quad D_s = \frac{EA}{\gamma U_e^2}$$
$$D_M = \frac{2\gamma}{\rho S_B} \quad D_R = \frac{S_B}{S_A}$$

where reference is made to the Nomenclature for the meaning of the symbols.

As usual in the linear stability analysis, Eqs. (1-12) were linearized, according to the small perturbation theory. The initial equilibrium situation corresponded in all the cases to trimmed steady level flight of the system. The scalar equivalent expressions of the equilibrium equations and of their linearized forms were then discretized following Satofuka's improved differential quadrature technique[(6)]. As a result of this last method and at the end of this step the equations which govern the state of the two planes have been implemented as boundary conditions of the equations for the cable.

More details on the discretization of these equations can be found in Ref. 7, but a few comments are to be made here. Essentially the adopted discretization method consists in dividing the continuous cable into N tracts by means of $N+1$ nodes. The values of the unknowns in the nodes are then interpolated through Lagrange-type polynomials in order to have a continuous representation. After introducing the interpolating expressions into the partial differential equations, the differential problem is transformed into a finite set of ordinary differential equations. We can then remark in advance that the eigenvalues of the linearized form of the set of ordinary differential equations include the finite number of those corresponding to the modes which are characteristic of the cable.

In the following section and for the sake of simplicity, we will not mention the higher order eigenvalues associated to the elastic behaviour of the cable since their sensitivities to the parameters of the system are practically zero.

As a final remark, before the presentation of the results we note that for the discussion of the influence of the considered parameters on the dynamics of the system we will follow the way which will appear more convenient from the point of view of the physics of the problem. In this respect use will be made either of the calculated sensitivities and/or of the root loci themselves whichever gives more ease in the interpretation of the results.

Turning now to the sensitivity matrix, the classical procedure for its evaluation can be summarized as follows. Let λ_i and $\mathbf{x}_i$ be the i-th eigenvalue and the associated *right* eigenvector of the state equation so that

$$\mathbf{A}\mathbf{x}_i = \lambda_i \mathbf{x}_i$$

and let $\mathbf{y}_i$ be the associated *left* eigenvector, i.e.

$$\mathbf{A}^T\mathbf{y}_i = \lambda_i^T \mathbf{y}_i$$

Since for $i \neq j$, $(\lambda_i - \lambda_j)\mathbf{y}_j^T\mathbf{U}\mathbf{x}_i = 0$, after normalization of the eigenvectors one has the following orthonormality relation

$$\mathbf{y}_j^T\mathbf{U}\mathbf{x}_i = \delta_{ij}$$

with δ_{ij} the Kronecker's delta.

Simple considerations lead to

$$\mathbf{y}_i^T(\lambda_i\mathbf{U} - \mathbf{A})\mathbf{x}_i = 0$$

and when we evaluate the derivative of this equation with respect to a parameter p upon which the state matrix depends we obtain the following expression

$$\frac{\partial \mathbf{y}_i^T}{\partial p}(\lambda_i\mathbf{U} - \mathbf{A})\mathbf{x}_i +$$
$$\mathbf{y}_i^T(\lambda_i\mathbf{U} - \mathbf{A})\frac{\partial \mathbf{x}_i}{\partial p} + \mathbf{y}_i^T\left(\frac{\partial \lambda_i}{\partial p}\mathbf{U} - \frac{\partial \mathbf{A}}{\partial p}\right)\mathbf{x}_i = 0$$

provided that the proper differentiability conditions are satisfied. From the definitions and the orthonormality condition this equation finally reduces to

$$\frac{\partial \lambda_i}{\partial p} = \mathbf{y}_i^T \frac{\partial \mathbf{A}}{\partial p}\mathbf{x}_i$$

This relation above allowed the numerical calculation of the sensitivities. Incidentally we just remark that great care has to be paid in the computation of the derivatives of $\mathbf{A}$ in correspondence with the branching points of the eigenvalues.

III. Results

A first discussion of some of the main parameters which influence the characteristic modes of a towed sailplane was presented in Ref. 1 for the longitudinal case, and in Ref. 3 for the general three-dimensional motion. In those papers, in particular, it was found that an important role for the stability analysis is played by the length of the cable, the vertical separation of the two planes, the speed at equilibrium, the position of the attachment point on the glider.

As in the references cited above we will proceed in the investigation of the sensitivity matrix by taking into account the dimensional form of the parameters and – therefore – of the eigenvalues and their derivatives. This was decided for the sake of practicality and immediate feeling of the results from the physical point of view.

Although a thoroughful exploration of the sensitivity elements with respect to geometric and kinetic parameters was carried out, we will show here only the most significant results. These results were obtained after chosing for the tug and for the glider the planes whose characteristic data are reported in Table 1. The data were taken from Ref. 8.

In the sequel we will firstly consider the sensitivity of the eigenvalues of the system in the vertical plane with respect to *i)* the angle of attack of the sailplane, *ii)* the horizontal and *iii)* the vertical displacement of the attachment point, *iv)* the length of the rope.

Since the dynamic characteristics of the system are in general complicated it is sometimes relatively difficult to realize the physical causes influencing the various modes. If we consider, for example, just the longitudinal case, the two planes when singularly examined present – as is well known – at fixed stick a phugoid mode and a short period mode. On the other hand, the cable alone will behave in many very different ways as a consequence of the actions and of the constrains which are imposed at the two ends. In this last case we will in general observe modes which depend upon the elastic characteristics of the rope and modes which correspond to the motions of an inextensible cable subjected to mass and aerodynamic forces. When the system is considered as a whole one can intuitively say that the original characteristic modes of each part should be distinguishable in most circumstances. This is of course true but there are cases where the modal interaction among the elements of the system is such that a more or less immediate interpretation of the modes is out of question. This happens in particular in the proximity of degenerate modes[9,10]. For these reason, as we shall see, it seemed proper to analyze the sensitivity to *v)* the elastic modulus of the cable and to *vi)* the minimum drag coefficient of the glider.

For motions out of the vertical plane, after a short discussion of the characteristics of the dynamics of the system, we will show the sensitivity to *vii)* the horizontal and the vertical displacements of the attachment point and to *viii)* the length of the rope.

In all the cases which will be presented herein the initial equilibrium conditions correspond to a uniform horizontal speed u_0 = 30 m/s, to sea level altitude and to an angle of attack of the glider equal to -0.007 rad. In the same conditions the locations of the attachment points are $\xi_A = -4.9$ m, $\zeta_A = 0.27$ m and $\xi_B = 2$ m, $\zeta_B = 0$ respectively. As for the cable data we have $\gamma = 4 \times 10^{-2}$ kg/m, $EA_c = 3.8 \times 10^4$ N, $k = 1.15$, $C_{D_{0_c}} = 0.02$, $l_0 = 50$ m.

The noticeable sensitivity of the system to the vertical separation of the two plane, Δz_B, will be expressed in terms of the derivative $\partial\lambda/\partial\alpha_B$, since - in equilibrium - there is a one to one correspondence between Δz_B and α_B, as shown in Fig. 2.

Motions in the longitudinal plane

We begin with the case of motions in the longitudinal vertical plane and, following Ref. 1, Fig. 3 shows the real part and the coefficient of the imaginary part of the eigenvalues versus α_B. We have two damped periodic motions and two aperiodic motions, one of which is sensibly unstable in all range of angles of attack. In this figure, as in all the following ones, two short period modes are not reported which are practically equal to the short period modes of each of the two planes. This is because their values are unaffected by variations of α_B. Mode 3 corresponds to the phugoid of the tug whereas the phugoid of the glider degenerates into the two aperiodic modes, Mode 1 and 2 respectively. Finally, Mode 4 has to be associated to the dynamics of the cable and is always damped. This last point will be discussed a little later.

After the necessary calculations we obtain the sensitivity with respect to α_B versus α_B which is reported in Fig. 4. Subsequently we present Fig. 5 which provides $\partial\lambda/\partial\xi_B$ versus α_B. A comparison of the two figures is meaningful in the sense that it immediately shows the relative inportance of the two parameters α_B and ξ_B in determining the response of our dynamic system to changes of the same quantity α_B. Although the functional dependences of $Im(\partial\lambda/\partial\alpha_B)$ and $Im(\partial\lambda/\partial\xi_B)$ upon α_B are pretty similar, the values of both the imaginary and the real parts of the two sensitivities differ by some orders of magnitude.

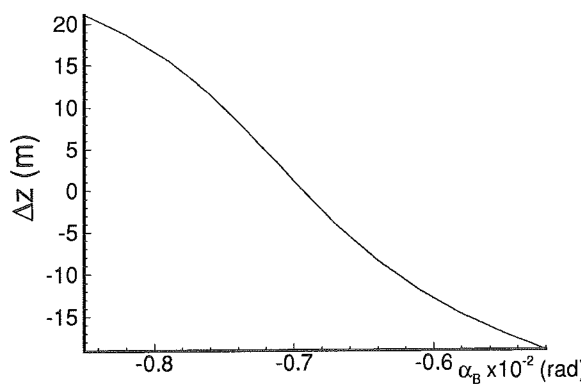

Fig. 2 - $\Delta z = z_{G_A} - z_{G_B}$ vs. α_B at equilibrium; $\xi_B = 2$m, $\zeta_B = 0$

It is significant to compare the sensitivities with respect to the position (ξ_B, ζ_B). Tables 2 and 3 list $\partial\lambda/\partial\xi_B$ and $\partial\lambda/\partial\zeta_B$ as functions of ξ_B and ζ_B respectively.

It is immediate to realize the greater influence of the vertical displacement of the attachment point on the eigenvalues rather than the one of the horizontal displacement. In both cases the sensitivities relative to Mode 3 which stems from the phugoid of the aircraft are negligible. Changes in

Table 1 - Tow-plane and glider data

Tow-plane	m = 800kg	I_ξ =1268 kgm²	I_η = 1800 kgm²
	I_ζ = 2630 kgm²	$I_{\xi\zeta} = 0$	
	b = 11m	S = 16m²	$A = 7.6$
Glider	m = 300 kg	I_ξ =1500 kgm²	I_η = 130 kgm²
	I_ζ = 200 kgm²	$I_{\xi\zeta} = 0$	
	b = 15 m	S = 13m²	$A = 17.3$

the vertical position of the attachment determine a variation of the damping coefficient of the elastic mode at a constant rate and influence the damping of Mode 1. Note that Modes 1 and 2 correspond to a couple of conjugated complex roots for negative values of ς_B, that is when the attachment point is located above the c.g. of the glider. In this condition the long period mode of the sailplane is recovered.

We pass now to the sensitivity with respect to the length of the rope. The results of the calculations are given in Table 4 and show that this last parameter influences only the frequency of the elastic mode, as one would have expected.

Since we are discussing the sensitivity to one of the parameters of the cable, it is worth entering in some more details concerning the modes which are more directly af-

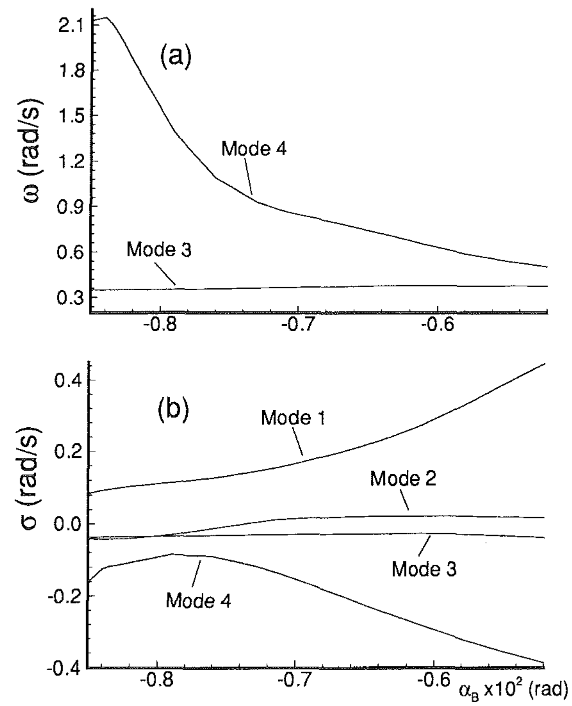

Fig. 3 - Real part (σ) and coefficient of the imaginary part (ω) of eigenvalues of Modes 1-4 vs. α_B; ξ_B = 2m, $\varsigma_B = 0$.

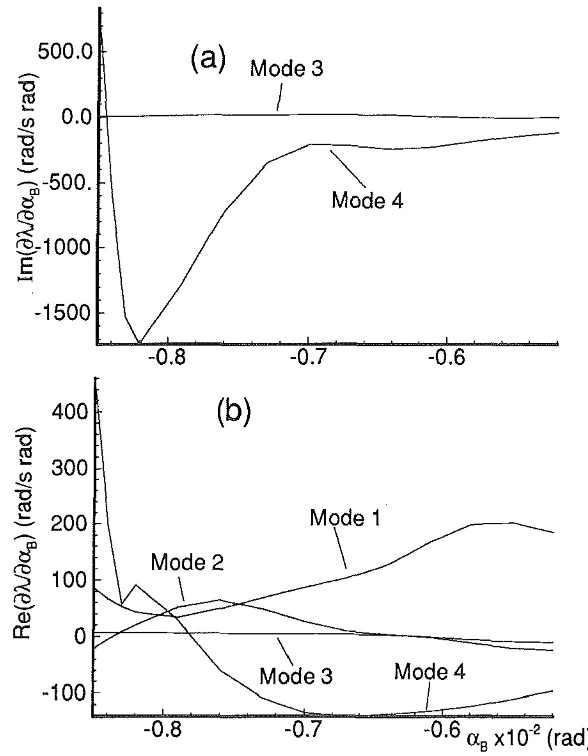

Fig. 4 - Real part and coefficient of the imaginary part of $\partial\lambda/\partial\alpha_B$ of Modes 1-4 vs. α_B; ξ_B = 2m, $\varsigma_B = 0$.

Table 2 - $\partial\lambda/\partial\xi_B$(rad/s m) vs. ξ_B; $\varsigma_B = 0$.

ξ_B (m)	Mode 1	Mode 2	Mode 3	Mode 4
1.6	-2.84 (-2)	3.45 (-2)	-4.90 (-3) -3.24(-3)i	-3.94 (-3) +1.87(-2)i
1.8	-2.84 (-2)	3.66 (-2)	-4.89 (-3) -3.07(-3)i	-5.10 (-3) +1.93(-2)i
2.0	-2.88 (-2)	3.92 (-2)	-4.86 (-3) -2.91(-3)i	-6.46 (-3) +1.89(-2)i
2.2	-2.99 (-2)	4.01 (-2)	-4.83 (-3) -2.72(-3)i	-7.52 (-3) +1.89(-2)i
2.4	-3.19 (-2)	4.56 (-2)	-4.81 (-3) -2.53(-3)i	-8.47 (-3) +1.90(-2)i

Table 3 - $\partial\lambda/\partial\varsigma_B$(rad/s m) vs. ς_B; $\xi_B = 2m$.

ς_B (m)	Mode 1-2		Mode 3	Mode 4
-0.4	2.04 (-1) -5.28 (-2)i		6.56(-3)-2.38(-3)i	-1.98(-1)-4.42(-2)i
-0.2	1.91(-1)-4.01i		3.91(-3)-3.57(-3)i	-1.96(-1)-2.40(-2)i
0	4.05(-1)	-3.96(-2)	1.85(-3)-3.61(-3)i	-1.94(-1)-1.37(-2)i
0.2	3.61(-1)	-2.10(-2)	3.29(-4)-2.80(-3)i	-1.91(-1)-1.28(-2)i
0.4	3.35(-1)	-1.06(-2)	5.90(-4)-2.23(-3)i	-1.91(-1)-1.28(-2)i

Table 4 - $\partial\lambda/\partial l_0$(rad/s m) vs. l_0 : ξ_B = 2m, $\varsigma_B = 0$

l_0 (m)	Mode 1	Mode 2	Mode 3	Mode 4
30	6.02(-3)	-5.73(-3)	8.11(-5)+3.82(-6)i	1.17(-2)-5.28(-2)i
40	1.96(-3)	-2.37(-3)	2.33(-5)-5.19(-5)i	3.88(-3)-2.90(-2)i
50	4.07(-4)	-1.20(-3)	-3.85(-6)-7.34(-5)i	1.80(-3)-1.75(-2)i
60	-2.82(-4)	-6.62(-4)	-1.86(-5)-8.20(-5)i	1.06(-3)-1.11(-2)i
70	-5.76(-4)	-3.81(-4)	-2.72(-5)-8.56(-5)i	7.27(-4)-7.39(-3)i

fected by the characteristics of the rope.

As we anticipated it is not immediate, in some cases, to understand what the behaviuor of the cable is. If we refer to the investigations in Ref. 10 and try to apply those results to the present circumstances, we already see that the response of the connection between tow-plane and sailplane can be extremely different in terms of frequency, and it depends on the geometric configuration of the cable (essentially on its curvature), on its physical characteristics and on the tension to which it is subjected.

First of all we note that, when we let the mass per unit length of the rope vanish, so that the rope itself reduces to an elastic massless link, the elastic mode has a frequency equal to $[EA_c(m_A + m_B)/lm_A m_B]^{1/2}$ which is sometimes called *bounce* frequency. In equilibrium the case system which we are considering here would have a bounce frecuency equal to 1.8 rad/s. For the same system, in Ref. 1, it was already shown that the values of the parameters are such that the frequencies which can be directly referred to the rope are far from this value of the bounce frequency.

Since in von Flotow's[10] analysis the great role played by the elastic modulus, the tension and the curvature are put into evidence, we present Fig. 6 and Table 5 in order to justify the distance between the values of the vibrational frequency of the cable and the bounce value. In particular Fig. 6 shows the elastic eigenvalue $Im(\lambda_4)$ versus E, whereas Table 5 reports $Im(\lambda_4)$ as a function of $C_{D_{0_B}}$, which is practically indicative of the tension at the glider's end of the cable.

Figure 6 clearly shows that, in a wide range of values of E, our system has a values of $Im(\lambda_4)$ which falls far from the bounce value. In addition, the functional relation between $Im(\lambda_4)$ and E does not follow the bounce frequency law. However Table 5 shows that, all the rest being kept constant, if we change the aerodynamic drag of the glider and, in so doing, the tension at the end of the rope, then a definite increase of $C_{D_{0_B}}$ drives the imaginary part of λ_4 towards the bounce value. Table 6 shows the sensitivity to E of the four considered modes, for two different values of the mass per unit length of the cable and for two different locations of the attachment point on the tug. We note that $\partial\lambda_4/\partial E$ is strongly affected by γ and increases to great values as $Im(\lambda_4)$ approaches the bounce value. On the other hand, the location of the attachment point on the aircraft (ξ_A, ζ_A) does not practically influence Modes 3 and 4 but changes a periodic phugoid motion of the sailplane - when the attachment is in the c.g. of the tug - into two aperiodic motions.

A further consideration is suggested by Fig. 6. Apart from its influence on the elastic behaviour of the cable, the elastic modulus noticeably affects the diverging motions of Modes 1 and 2.

Motions out of the longitudinal plane

A rather extended investigation of the out of plane dynamics of a tug–rope–sailplane system was presented in Ref. 3. The guidelines of that research were based on the same full model for representing the behaviour of the cable which is adopted in this paper. Following that analysis we will consider here the main aspects of the lateral and directional stability characteristics and we will discuss the sensitivity of the system to the principal intervening parameters.

When the state equation for the lateral dynamics is considered, some of the eigenvalues of the state matrix can be associated to already familiar modes. In fact one obtains two couples of conjugates complex roots which correspond

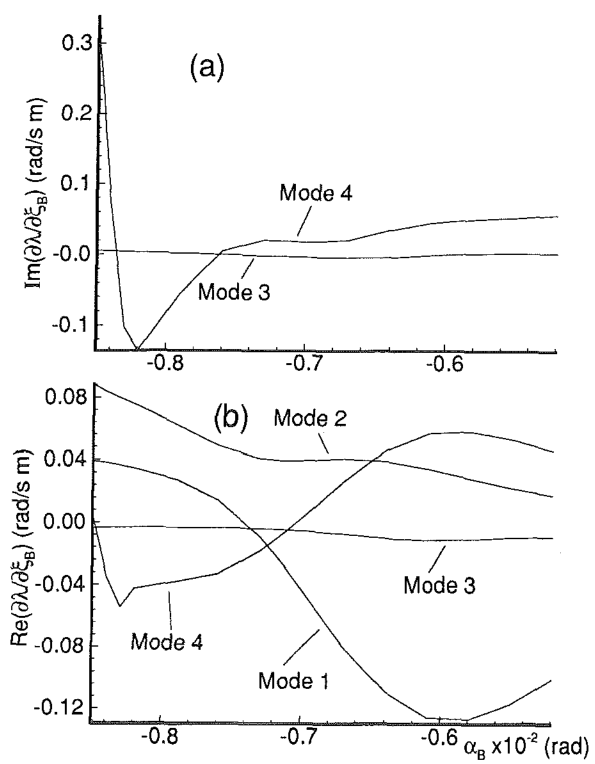

Fig. 5 - Real part and coefficient of the imaginary part of $\partial\lambda/\partial\xi_B$ of Modes 1-4 vs. α_B; $\zeta_B = 0$.

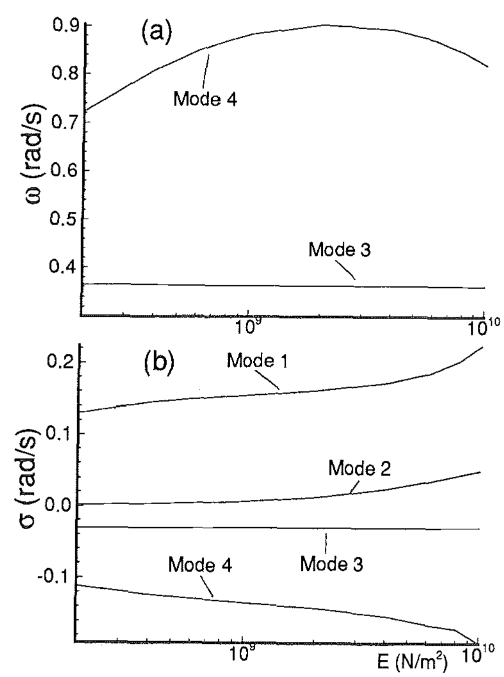

Fig. 6 - Real part (σ) and coefficient of the imaginary part (ω) of eigenvalues of Modes 1-4 vs. E: $\xi_B = 2$ m, $\zeta_B = 0$.

to the dutch roll modes of tow–plane and glider respectively. Other two real roots can be assigned to the roll motions of the two planes. A second aperiodic motion is in any case present and corresponds to the spiral mode of the sailplane.

Typically, a couple of conjugate complex roots is now found which can be interpreted as a long period oscillation of the system as a whole. The real part of these eigenvalues can be either positive or negative and the corresponding motion can be either amplified or damped depending on the locations of the attachment points. The frequency of this oscillation is of an order of magnitude smaller than the dutch roll frequencies. Whereas, as we said, one root can be made to correspond to the spiral motion of the glider, a second real root appears to characterize an aperiodic motion of the entire system. In addition to the modes indicated above, other roots are associated to the dynamics of the cable. Analogously to what happens in the in–plane dynamics, after the cable is discretized by means of $N+1$ nodes, $N-2$ conjugated roots are joined to the modes of the rope.

In this paper we will report and discuss the first vibrational mode which is the only elastic mode whose frequency may be comparable to the other frequencies of the system. In fact, we will deal only with those modes which can be influenced by the fundamental parameters of the system like the ones which were treated in the in–plane case. Therefore the sensitivities of the dutch roll and of the roll motions of the two planes will not be treated anymore. Just as an example of insensitivity we refer that, for the single aircraft and the single sailplane, the dutch roll frequencies are $\lambda_{DR_A} = -4.91 \times 10^{-1} \pm 1.68i$ rad/s and $\lambda_{DR_B} = -4.84 \times 10^{-1} \pm 1.63i$ rad/s, whereas in the case of the complete system we have the roots $\lambda_{DR_A} = -4.78 \times 10^{-1} \pm 1.73i$ rad/s and $\lambda_{DR_B} = -4.75 \times 10^{-1} \pm 1.74i$ rad/s. For the roll modes the differences are even more negligible.

In what follows and in Fig. 7 the considered modes will then be: 1) the spiral mode of the sailplane, 2) the aperiodic motion of the system, 3) the long period mode of the system, 4) the first elastic lateral vibration.

If we begin with the sensitivity to the horizontal position of the attachment point on the glider, the influence of variations of this parameter on the Modes 3 and 4 is negligible. Some influence is present on the spiral motion. The value of σ_1 is increased from 9.04×10^{-3} rad/s to 1.10×10^{-2} for ξ_B moving from the c.g. to the nose of the sailplane. For the same displacement of ξ_B the value of σ_2 passes from 1.81×10^{-1} rad/s to 1.42×10^{-1} rad/s. All this means that for ξ_B moving forward, the spiral motion of the glider becomes a little more diverging whereas the aperiodic motion of the system becomes less divergent.

When the vertical location ς_B is considered, the influence of this parameter does not practically affects Modes 1 and 2. The spiral mode of the glider is also not influenced as ς_B moves from below to above the c.g., whereas σ_2 increases from 1.42×10^{-1} rad/s to 1.55×10^{-1} rad/s as ς_B goes from 0.5 m to -0.5 m, respectively.

The last sensitivities which will be considered are those to the length of the rope. Figure 7 shows the main results. If we begin our discussion with the first elastic lateral vibration, an approximate expression of its frequency is given by the relation for the first frequency of an elastic cable

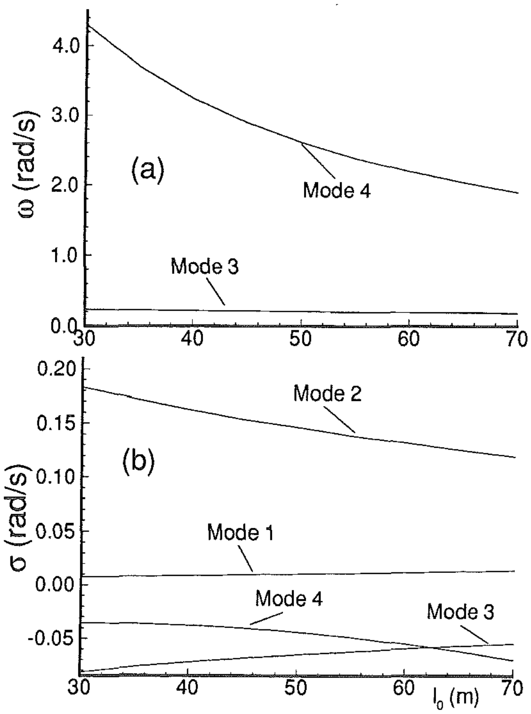

Fig. 7 - Real part (σ) and coefficient of the imaginary part (ω) of eigenvalues of the lateral Modes 1-4 vs. l_0: $\xi_B = 2$ m, $\varsigma_B = 0$.

Table 5 - λ vs. $C_{D_{O_B}}$; $\xi_A = \varsigma_A = 0$: $\xi_B = 2$m, $\varsigma_B = 0$

$C_{D_{O_B}}$	Mode 1-2	Mode 3	Mode 4
0.006	$9.24(-3) \pm 1.34(-1)i$	$-1.18(-2) \pm 3.58(-1)i$	$-3.47(-1) \pm 8.88(-1)i$
0.008	$4.00(-3) \pm 1.51(-1)i$	$-2.04(-2) \pm 3.58(-1)i$	$-3.31(-2) \pm 1.06i$
0.015	$-7.44(-3) \pm 1.95(-1)i$	$-2.66(-2) \pm 3.58(-1)i$	$-3.17(-2) \pm 1.51i$
0.030	$-1.60(-2) \pm 2.63(-1)i$	$-4.78(-2) \pm 3.53(-1)i$	$-3.53(-2) \pm 1.81i$
0.060	$-1.06(-3) \pm 3.17(-1)i$	$-1.16(-1) \pm 3.89(-1)i$	$-5.10(-2) \pm 1.89i$

Table 6 - $\partial\lambda/\partial E \times 10^{10}$(rad m^2/Ns) vs. γ : $\xi_B = 2$m, $\varsigma_B = 0$.

γ (kg/m)	Mode 1	Mode 2	Mode 3	Mode 4	
0.04	9.29(-2)	6.29(-2)	-1.39(-3)-2.08(-3)i	-1.01(-1)+5.08(-1)i	$\xi_A =$ --4.9m
0.002	1.82(-2)	4.53(-3)	1.90(-4)-5.92(-4)i	-2.17+9.63i	$\varsigma_A = 0.27$m
0.04	3.17(-2)+4.06(-2)i		-2.25(-4) -2.59(-4)i	-3.78(-2)+5.10(-1)i	$\xi_A = 0$
0.002	2.89(-3)+2.71(-2)i		-2.07(-4)-5.86(-5)i	-2.88(-2)+9.02i	$\varsigma_A = 0$

with fixed end points, i.e. $\omega_4 \simeq \pi(|g|/8f)^{1/2}$ where f is the sag. This simple equation provides an immediate means for evaluating the influence of the curvature of the cable and, therefore, of l_0 too. Apart from this initial consideration we note from Fig. 7 also that Mode 4 is the most sensitive to changes in l_0. However what seems to be the most beneficial effect of an increasing rope length is the reduction of the amplifying coefficient σ_2 relative to the aperiodic motion of the system. The associated sensitivity $\partial\sigma_2/\partial l_0$ is decreasing with l_0. From the same figure we see that an increasing length determines a relatively small increase of the spiral motion amplification.

IV. Conclusion

In this work the capabilities of a rigorous representation of the dynamics of the single elements of a tug–rope–glider system were shown in connection with the evaluation of the influence of the system parameters on the stability. The whole investigation of the sensitivity matrix took advantage by the consistency of the physico–mathematical model and by the effectiveness of the discretization procedure which was adopted for reducing a problem governed by partial differential equations to a finite set of ordinary differential equations.

The numerical calculations were carried out for motions in and out of the vertical longitudinal plane. The main results concern a distinction between parameters which influence the dynamics of the system and parameters which do not. Among the first ones evidence was given to the glider angle of attack, the length of the cable and the location of the attachment point on the sailplane.

The approach to sensitivity calculations in the peculiar situation which was considered as case study can help further investigations in applications connected with the dynamics and safety of the flight of analogous towed systems.

References

1. de Matteis G., "Dynamics of a Towed Sailplane", AIAA Paper 91-2862, in press in the Journal of Guidance, Control and Dynamics.
2. Adelman H.M., Haftka R.T., "Sensitivity Analysis in Engineering", NASA CP 2457, 1987.
3. D'Ambrosio D., "Sailplane Dynamics during Towing" (in Italian), Thesis, University of Rome, 1992.
4. De Laurier J.D., "A First Order Theory for Predicting the Stability of Cable Towed and Tethered Bodies where the Cable has a General Curvature and Tension Vibration", von Karman Institute, Tech. Note 68, 1970.
5. Etkin B, *Dynamics of Atmospheric Flight*, John Wiley & Sons, Inc., New York, 1972.
6. Satofuka N., "A New Explicit Method for the Numerical Solution of Parabolic Differential Equations", in *Numerical Properties and Methodologies in Heat Transfer* (T.M. Shih, Ed.), Hemisphere Publ., Washington, 1983, pp. 97-108.
7. de Matteis G., de Socio L.M., "A Discretized Model for the Dynamics of a Tethered Satellite System and Applications", Mathematical Models and Methods in Applied Sciences, vol. 1, no. 3, 1991, pp. 377-398.
8. Morelli, P., *Static Stability and Control of Sailplanes*, O.S.T.I.V., Voorburg, The Netherlands, 1976.
9. Afolabi, D., "Model Interaction in Linear Dynamic Systems Near Degenerate Modes", NASA TM–105315, ICOMP–91–21, 1991.
10. von Flotow, A.H., Wereley, N.M., "Insight and Approximations in Dynamic Analysis of Spacecraft Tethers", *Mechanics and Control of Large Space Structures*, J.L. Junkins Ed., AIAA Progress in Astronautics and Aeronautics, Washington, 1990, pp. 667–696.

Acknowledgement

This work was partially supported by the Italian Ministry of University and Technological and Scientific Research.